Available online at www.jourcc.com

Journal homepage: www.JOURCC.com

Journal of Composites and Compounds

Theoretical Electrochemical Study and Calculation of Free Energies of Electron Transfer in β-Cyclodextrins/Fullerenes C_{60} Nanostructure Complexes

Bahareh Farasati Far [a], ***Mohammad Reza Naimi-Jamal*** [a], ***Mohammad Rizehbandi*** [b]*, ***Muhammad Yasir Mehboob*** [c]

[a] *Research Laboratory of Green Organic Synthesis and Polymers, Department of Chemistry, Iran University of Science and Technology, Tehran, Iran*

[b] *Chemistry Department, Faculty of Science, Guilan University, Guilan, Iran*

[c] *Department of Chemistry, University of Okara, Okara-56300, Pakistan*

A B S T R A C T

Cyclodextrin is a cyclic molecule that contains the three essential six, seven, and eight glucose molecules, called by the names α, β, and γ-cyclodextrin, individually. Cyclodextrins are thought to be completely polar as a result of the hydroxyl groups presents in glucose moieties. Secondary C_2-hydroxyl groups of glucose units are found on the secondary face, while the C_6-hydroxyl type groups are located on the primary face because these are related to the primary face of the incomplete cone. The C_1 group, a glucoside oxygen ring, and another ring of C-H groups make up the inside of the cyclodextrin cone, making it rather nonpolar. Hydrophobic fullerenes C_n [n= 60, 70, 76, 82, and 86] have been chosen for the guest molecules and different parameters like first to fourth free activations, the kinetic rate constant, the energies of electron transfer ($k_{et(n)}$), and $\Delta G^{\#}_{et(n)}$ where (n=1-4), were calculated and discussed in detail. All the computed results showed the best coherence with the Marcus theory. Different analyses suggested that free energy is lowered due to an efficient electron transfer, which begins with the first step (the first of the four activate free energy values).

Peer review under responsibility of UGPH.

A R T I C L E I N F O R M A T I O N

Article history:
Received xx December 20xx
Received in revised form xx December 20xx
Accepted xx December 20xx

Keywords:
Fullerenes
β–Cyclodextrins
The electron transfer energies
Rate constants
Marcus theory

Table of Abbreviations

CT	The Charge transfer
LE	Locally energized
PLS	Partial least squares
QMD	Quantum molecular dynamics
QSAR	Quantitative structure-activity relationship
QSPR	Quantitative structure-property relationship
SWCNT	Single-walled carbon nanotubes

1. Introduction

In the pharmaceutical industry, appropriate materials as a carrier are employed to decrease the unfavorable qualities of drug molecules; while designing enhanced dosage forms [1]. Cyclodextrins are cyclic oligosaccharides with a surface hydrophilic and a core lipophilic cavity that form inclusion complexes with molecules to change their physical, chemical, and biological properties. Therefore, as a pharmaceutical excipient, β-Cyclodextrin (β-CD) has been included in pharmaceutical formulations. Because of β-CD's capacity to boost the solubility and stability of pharmaceuticals by forming solid-state complexes, Cyclodextrins frequently employed in the pharmaceutical industry [2, 3]. Additionally, cyclodextrins can minimize gastrointestinal drug sensitivity, convert liquid drugs to crystalline or amorphous powders, and avoid drug-drug and drug–excipient interactions [4].

Seven D-(+)-glucopyranose monomers are combined and produce 2-hydroxypropyl-β-cyclodextrin, a cyclic oligosaccharide with increased water solubility of numerous compounds, including those that have a phenyl group. Structural units of cyclodextrins are made up of 5 or more types of α-D-glucopyranoside, such as attilosis (a structure of starch) [5]. Different kinds of cyclodextrins contain a variety of glucose monomers (with six to eight units per ring) which are the most common ones. Complete hydrolysis of starch produces the sugar D-glucose, or dextrose, as it is more frequently known. Soluble starch, maltose, and different dextrins have all been mentioned. Saccharide is produced

* *Corresponding author: Mohammad Rizehbandi; E-mail: Rizehbandi.mohammad@yahoo.com*

https://doi.org/10.52547/jcc.5.2.3

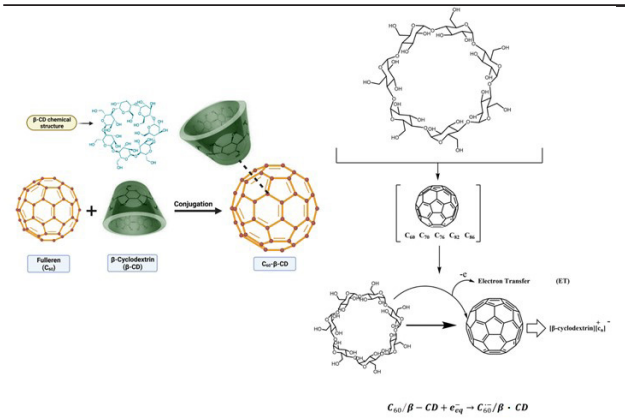

Fig. 1. The conjectured structures model for fullerene (n) with β-CD. (n= 60, 70, 76, 82, and 86) which create [β-CD].Cn. The theoretical electron transfer has been shown separately between the β-CD (1-4) and fullerens.

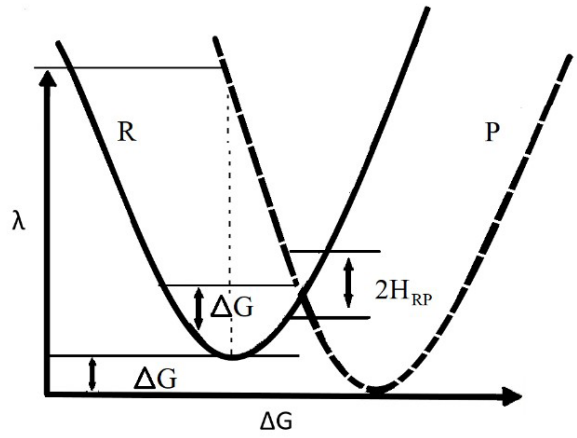

Fig. 2. The concentration on the β-CD and electron transfer with fullerenes. The imaginary ET process between β–CD, and fullerenes has been demonstrated separately.

by the enzymatic hydrolysis of starch [6]. Chemically, β-CD has a hydrophobic interior and a hydrophilic exterior and is commonly used in pharmaceuticals and industrial goods for its ability to improve the bioavailability and solubility of guest compounds [7] Such examples are hydrocortisone [8], prostaglandin [9], nitroglycerin [10], itraconazole [11], and chloramphenicol [12]. Cyclodextrin maintains solubility and stability for these drugs. β-CDs also act as prebiotics. Supplementing with β-CD may also improve intestinal health and immunity, as populating the gut with beneficial microbes has improved intestinal health and immunity. Although most hydrophobic molecules are unable to permeate the body's tissues, cyclodextrins with these compounds can penetrate the body's tissues and are thus helpful for transporting active biomolecules in a specific area [13]. Alternatively, complexes can be disrupted by heating or the activity of enzymes capable of cleaving the α -1,4 links between glucose monomers. Cyclodextrins have also been shown to enhance the mucosal penetration of drugs [14].

Electrochemically, fullerenes like C_{60} are easy to reduce but challenging to oxidize. Therefore, they're classified as electrophiles or electron acceptors instead of nucleophiles or electron givers. As a result, polar reactions with a range of nucleophiles have been used to derivatize fullerenes. Due to its unique qualities, including its electron donor or acceptor capability and photophysical and photochemical behavior, fullerene is widely regarded as a potent building block in material sciences and medicinal chemistry [15, 16]. The Diels–Alder reaction of C_{60} with anthryl-β-CD is used to synthesize the β-CD -C_{60} complex conjugated in this paper. Even though it is [4+2], cycloaddition is one of the most efficient ways for the selective synthesis process of C_{60} fullerene at the 6,6-ring junctions.

Table 1.
The link between the Cn index of fullerenes and the one to four free-energy values of transfer of electrons is represented by the second-order polynomial equation (ΔGet(n).

$\Delta G_{et(n)}$ *of* [β-CD].C_n		$\Delta G_{et(n)}=a(n)^2+b(n)+c$		
n	R^2	A	B	C
1	0.987	-0.0235	2.9196	-52.2080
2	0.992	-0.0281	3.5028	-61.8920
3	0.938	-0.0025	0.0081	66.1910
4	0.947	-0.0039	0.1112	75.5480

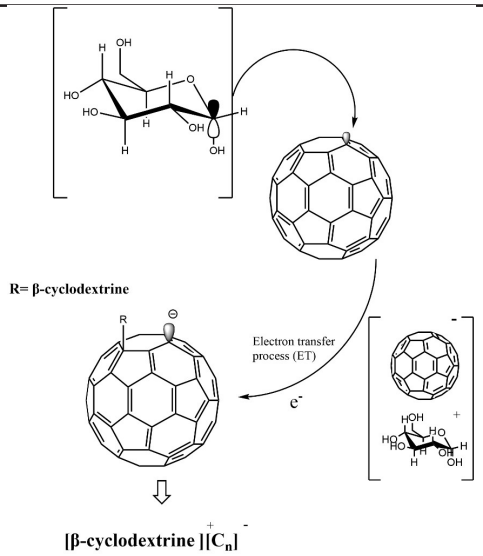

Fig. 3. Diagram of potential levels of reactants and products.

The quantitative structure-activity relationship (QSAR) and the quantitative structure-property interaction are both successfully determined by graph theory (QSPR). In this regard, over 3000 topological graphs indices are registered in Chemical Databases of high significance all over the universe. Perhaps the Wiener index is the best known and most widely dependent on the topological vertices distances in the respective graph [17]. QSAR creates correlations between a compound's structural features or characteristics and a molecular response derived from experimental data to support molecular design. Physical property is a property of matter that has nothing to do with its chemical composition [18]. Excellent mathematical approaches build good relationships between various chemical properties [19]. Modeling performance should be assessed based on validating model predictions and acceptability of predictions for untested compounds using validation criteria that ensure the credibility of created QSAR models and give acceptance to predictions for compounds that have not been screened, presented in **Figure 1.** Using QSAR modeling is a continuous approach to minimizing the anticipated residues of the substances under investigation. The carbon atoms involved in the structure of fullerenes were considered in this study to address this. The Rehm-Weller equation (Eq.1) is used to calculate the free energy of electron transfer (ΔG_{et} (n); n=1–4) for supramolecular Fullerene C_n complexes. The calculations for the four reduction potentials are proposed (Red.E1 to Red.E4).

Many types of research focused on the physicochemical and mechanical properties of empty fullerenes and their internal angles [20]. In this research, the 4 free electron transfer energies (ΔG_{et} (1) to ΔG_{et} (4)) for β-CD supramolecular complexes of these electron transfer radicals have been calculated for the combination of the drug with C_{60} to C_{300} fullerenes. The activation energies of electron transfer and the kinetic rate of electron transfer constant are of the four reduced potential energies (Red.E1 to Red.E4) of fullerenes reported for (C_{60}, C_{70}, C_{76}, $C_{82,}$ and C_{86}), respectively. The data used in the graph drawing are from C_{60} to C_{86} fullerenes. Using the number of carbon atoms in this way, accompanied by the equations derived from this model, could be a reasonable

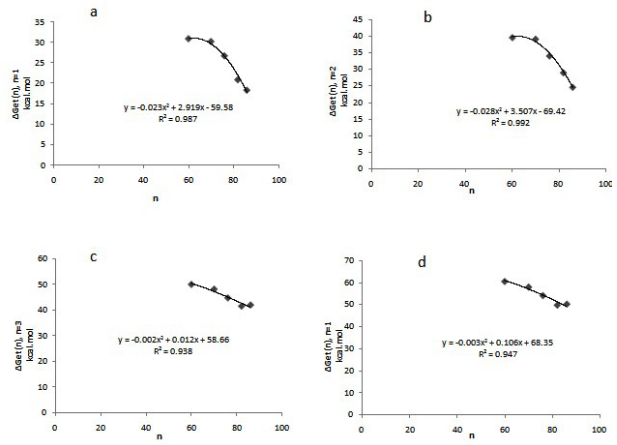

Fig. 4. A simple co-relation among the carbon atoms in fullerene and one to four free-energy of the ET process (ΔGet(n), n=1–4) of [β –CD]. Cn (C60, C70, C76, C82, and C86), compound complexes have structures similar to a, b, c, and d, [β –CD]. Cn.

structural relationship between the physical and chemical information mentioned. By using the equations in this method with an appropriate approximation, $\Delta G_{et}^{\#}$ (1) to $\Delta G_{et}^{\#}$ (4)) can be used for the nano-complex structure of β-CD and fullerenes (C_{60} to C_{300}).

The compressed mechanical features of fullerene molecules have been studied using quantum molecular dynamics (QMD), and in this study C_n where (n=60, 70, 76, 82, 86, 78, 84, 120, 132, 140, 146, 150, 160, 162, 240, 276, 288 and 300) [20]. Carbon-based compounds, such as fullerenes, were discovered due to unique molecules such as C_{70} and C_{60}. The electrochemical properties of fullerenes C_{60} were investigated before 1990, when they were first usable in microscopic quantities [21, 22]. After discovering the C_{60} structure, As a new hybridization method, the arranging of molecules in capsules for molecule-molecule or SWCNT (Single-walled carbon nanotubes) molecule interaction has been investigated [23]. It has already been shown that electrochemical methods (cathodically method) in dichloromethane reduce C_{60} to C_{60}^{-1}

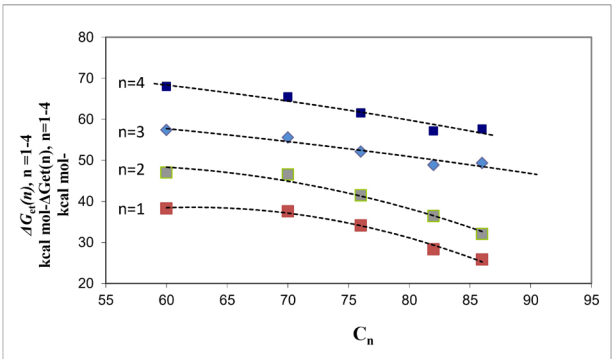

Fig. 5. The 1st, 2nd, 3rd, and 4th free energies of electron transfer is all related to the number of carbon atoms in fullerenes (n). Obtain(n) ΔGet (n = 4-1) connects to the Cn complex with β-CD.

and C_{60}^{-2} [24]. According to the orbital analysis of C_{60}, the LUMO (the lowest unoccupied molecular orbital) can take up to six electrons to create C_{60}^{-6}. Cathode reduction of C_{60} is performed in six single-electron reversible steps with −0.97 V vs. F_c/F_c^+ (F_c = ferrocene) to create C_{60}^{-6}.

Regarding fullerenes' incapacity to perform anodic electrochemistry, some fullerene substructures are well known to have electronic features similar to their aromatic analogs. Hence, this fact matches the electronic fullerene's structure. Because the resulting C_{60} anions (such as C_{60}, C_{260}, or C_{360}) have remarkable stability compared to other multiply charged organic ions, multiple and bidirectional electron additions are conceivable. The HOMO (highest occupied molecular orbital) cannot be forcefully doped using electrochemical conditions [25]. In the presence of a photon, a molecule can undergo a physical transformation that consists of an electron jumping from a ground state to a higher-energy orbital. Electrons in the ground-state orbital are then allowed to fill this empty ground-state orbital with an electron donor [26] An electron is generated in a high-energy orbital. It can be supplied to another electron acceptor [27, 28] reaction where electrons are transferred due to the application to a particular substance that possesses photoactive properties, such as semiconductors which can be photo-activated, for example, in solar cells, photosynthesis, some molecular complexes presented in Figure 2

Table 2.

The data coefficients of the macrocycles β-CD and the free energy of electron transfer (ΔGet) between Macrolides in kcal.mol–1.

Row	C_n	β -CD			
		$\Delta G_{et(1)}$*	$\Delta G_{et(2)}$*	$\Delta G_{et(3)}$*	$\Delta G_{et(4)}$*
A	C_{60}	31.06	39.86	50.34	60.98
B	C_{70}	29.74	38.40	47.19	57.07
C	C_{76}	26.69	34.83	45.06	54.36
D	C_{82}	21.95	29.24	42.75	51.38
E	C_{86}	17.85	24.39	41.10	49.23
F	C_{78}	25.30	33.19	44.31	53.40
G	C_{84}	19.99	26.92	41.94	50.32
H	C_{120}	-47.33	-53.16	23.89	26.08
I	C_{132}	-83.29	-96.04	16.43	15.79
J	C_{140}	-111.02	-129.12	11.05	8.33
K	C_{146}	-133.80	-156.29	6.80	2.41
L	C_{150}	-149.92	-175.53	3.87	-1.69
M	C_{160}	-193.50	-227.56	-3.81	-12.48
N	C_{162}	-202.79	-238.64	-5.41	-14.73
O	C_{240}	-711.25	-846.09	-83.41	-126.29
P	C_{276}	-1042.28	-1241.76	-129.74	-193.47
Q	C_{288}	-1166.15	-1389.83	-146.64	-218.06
R	C_{300}	-1296.78	-1546	-164.26	-243.76

[29-31].

Considering Figure 3, we can find the general schematic of the fullerene structure with cyclodextrin. Electron transfer energy between selected facilitators and fullerene structures can also be imagined. In Figure 3, the conjugation between β-CD and fullerenes C_n (C_{60}, C_{70}, C_{76}, $C_{82,}$ and C_{86}) creates [β–CD]@C_n complex.

In a study by Taherpour et al., structural relationships and theoretical study of the free energies of electron transfer, electrochemical properties, and electron transfer kinetics of cephalosporin antibiotics derivatives with fullerenes in the nanostructure of [R].C_n (cefadroxil, cefepime, cephalexin, cefotaxime, cefoperazone, and ceftriaxone) supramolecular complexes have been conducted. Results showed the photo-electron transfer process to find more medicinal activity properties for the cephalosporin antibiotics 1–6 in the presence of the selected fullerenes by performing the supramolecular complexes [cephalosporin antibiotics 1–6]C_n. The cephalosporin–fullerene supramolecular complexes and the calculated values of $\Delta G_{et}(n)$, $\Delta G^{\#}$ and $k_{(n)}$ (n = 1–4) corresponding to these complexes also have not been reported before [32].

In another study by Taherpour et al., free energies of electron transfer, electron transfer kinetic theoretical and quantitative structural relationships, and electrochemical properties studies of gadolinium nitride cluster fullerenes $Gd_3N@C_n$ in [X-UT-Y][$Gd_3N@C_n$](n = 80, 82, 84, 86 and 88) supramolecular complexes have been evaluated. The electron transfer between C_{80}, C_{82}, C_{84}, C_{86} and C_{88} derivatives such as nitride Gadolinium cluster [$Gd_3N@C_{80}$ (n = 80, 82, 84, 86 and 88)] and other molecules is thought to involve the transfer of electrons between molecules surrounding the fullerene cage. One of the most important classes of electron-transfer molecules is the [X-UT-Y][$Gd_3N@C_n$](n = 80, 82, 84, 86 and 88). The supramolecular complexes [X-UT-Y] 1–9 and $Gd_3N@C_{80}$ (n = 80, 82, 84, 86 and 88) possess a previously unreported host-guest interaction for electron transfer processes. The unsaturated, cis-geometry, thiocrown ethers, (1–9), (described as [X-UT-Y], where X and Y indicate the numbers of carbon and sulfur atoms, respectively), are a group of crown ethers that display interesting physiochemical properties in light of their conformational restriction compared to a corresponding saturated system, as well as the sizes of their cavities has been conducted [33].

Based on previous DFT studies, functionalized carbon nanotubes, and fullerenes can be used as nano vectors for drug delivery of antitubercular compounds. Results from the binding energies of boron nitride clusters indicate that it is possible thermodynamically to bind isoniazid to functionalized carbon nanotubes and functionalized fullerenes covalently, it being easier to bind isoniazid to functionalized fullerenes than to functionalized carbon nanotubes. From solvation energies calculations, the solubility of functionalized carbon nanotubes is higher than functionalized fullerenes, and both dissolutions in water are thermodynamically favorable [34].

The innovative aspect of our study is that topological indices have been successfully used to construct mathematical methods that relate structural data to various chemical and physical properties in pharmaceutical fields [35, 36]. In this study, to establish a good relationship between the cyclodextrins and fullerenes structures, the relationships between this index and oxidation potential (oxE1), as well as the first and second free energies of electron transfer (ΔG_{et} (n), for n = 1, 2, which is given by the Rehm-Weller equation) has been conducted.

2. Graphs and the mathematical method

A way of generating mathematical or computational models employing chemometrics approaches such as partial least squares (PLS) is known as a quantitative structure-activity relationship, which attempts to create a meaningful statistical relationship between structure and function. It's a principal component regression-related statistical approach. It finds a linear regression model by projecting the predicted and observed variables to a new space rather than finding hyperplanes of maximum variance between the response and independent variables.

Many researchers have used topological indicators for effective construction and helpful mathematical approaches for determining the

Table 3.
Values of data coefficients of macrocycles β-CD and free energy of electron transfer (ΔGet) between supramolecules in kcal mol–1.

		β-CD			
Row	**Formula of**	$\Delta G_{et(1)}^{\#}$	$\Delta G_{et(2)}^{\#}$	$\Delta G_{et(3)}^{\#}$	$\Delta G_{et(4)}^{\#}$
A	C_{60}	43.98	62.30	96.16	133.58
B	C_{70}	41.15	61.47	86.26	119.11
C	C_{76}	34.96	52.60	79.87	109.58
D	C_{82}	26.34	40.10	73.21	99.54
E	C_{86}	19.87	30.62	68.64	92.61
F	C_{78}	32.30	48.76	77.67	106.29
G	C_{84}	23.13	35.41	70.95	96.09
H	C_{120}	39.35	52.32	29.27	33.78
I	C_{132}	148.68	204.28	17.84	16.96
J	C_{140}	280.85	389.61	11.14	8.35
K	C_{146}	420.62	586.20	6.96	3.67
L	C_{150}	536.52	749.61	4.65	1.54
M	C_{160}	920.36	1.2910^{+3}	0.79	0.29
N	C_{162}	1.0110^{+3}	1.4310^{+3}	0.39	0.82
O	C_{240}	1.3310^{+4}	1.9010^{+4}	149.16	371.43
P	C_{276}	2.8910^{+4}	4.1210^{+4}	393.65	920.06
Q	C_{288}	3.6310^{+4}	5.1710^{+4}	511.79	1.1810^{+3}
R	C_{300}	4.4910^{+4}	6.4010^{+4}	654.65	1.4910^{+3}

link between these complexes' structural and physical data characteristics [29-31]. The fullerenes with a different number of carbons (C_n) were used as a structural indicator to quantify the number of carbons in these substances [33]. All calculations and graphs were done in MATLAB-7.4.0 (R2007a). To analyze the numerous beneficial qualities of the fullerenes, the number of carbons in the C_n fullerenes must be considered. In addition, electron transport theory was used in this investigation [38]. The free energy changes between an electron donor (D) and an electron acceptor (A) are calculated using the Rehm-Weller equation (Eq. 1):

$$\Delta G_{et}^{\circ} = e[E_D^{\circ} - E_A^{\circ}] - \Delta E^{*} + \omega_1 \quad \text{Eq . 1}$$

e: electric charge

ED°: Potential reduction of electron donor

EA°: Potential oxidation electron acceptor

ΔE *: Excited-state singlet or triplet energy

ω_1: Work required to enter a range of donors and acceptors electron transfer.

ED° and EA° denote the electron donor and acceptor reduction potentials; accordingly, E* signifies the energy of the excited singlet or triplet state, and 1 represents the work necessary to move the donor and acceptor nearer to the electron transfer (ET) gap. This formula has a zero-work factor if an electrostatic complex forms before the ET process. Marcus' electron transfer theory predicts a weak (0.05 eV) electrical connection between the initial locally energized (LE) and final charge transfer (CT) states, with the transition state located around the point in which the LE and CT terms cross [35]. The value of the electron transfer rate constant k_{et} is determined by the activation of free energy $\Delta G^{\#}_{et}$, which is a function of the reorganization energy (L/4) and the electron transfer driving force ΔG_{et} (Equation 2):

$$\Delta G^{\#} = L(1+\frac{\Delta G^{0}}{L})^{2} \quad \text{Eq . 2}$$

$\Delta G^{\#}_{et}$: The activation of free energy

(L): The reorganization of 'energy's function

ΔG°: the total free energy of Gibbs

$$K_{et} = Aexp(\frac{-\Delta G^{\#}}{k_b T}) \rightarrow \overrightarrow{\leftarrow} K_{et} = Ae^{\frac{-(\Delta G+L)^2}{4LRT}} \quad \text{Eq . 3}$$

$\Delta G^{\#}_{et}$, The activation of free energy

k_b: Boltzmann constant

H_{PR}: pair of electron intensity between the initial and final surfaces

k_{et}: electron transfer velocity

Organic molecules have a reorganization energy of between 0.1 and 0.3 eV. We used the smallest value of reorganization energy possible in our study [39]. Planck's formula is used to estimate the wavelength of an electromagnetic photon ($\lambda_{(n)}$; n=1-2) of the supramolecular nanostructure complexes used in the electron transfer process as follows:

$$\Delta G^{\#}_{et} = (l/4)(1+\Delta G_{et}/l)^{2} \quad \text{Eq. 4}$$

The Marcus theory, devised by Rudolph A. Marcus in 1956 to describe the rates of electron transfer processes, is used to determine the energy of restructuring [37]. This hypothesis explains the velocity of the transfer of electrons. An electron donor and an electron acceptor are involved in electron transfer, one of the most significant chemical reactions. When this happens, all valence electrons on the much more electropositive element are eliminated, revealing the atom's core. Marcus' hypothesis, which is based on the Arrhenius equation, has two approaches to determining the rate of chemical reactions: the 1st method is to obtain a formula for determining an indicator based on the initial definition of the electron equation that the electron pair of electrons between the primary and final surfaces in electron transport is presented in two ways [40]:

The first method to obtain a formula for determining an index is based on the initial definition of electronic coupling between the beginning and final levels in electron transport is described by the Arrhenius equation (Eq. 3). (e.g., the electron's overlap waves or parabolic diagram). In this regard, the k_{et} electron transfer velocity, the H_{PR} pair of electron intensity between the initial and final surfaces, ΔG^{o} is the total free energy of Gibbs, k_b Boltzmann constant, and λ energy of structure change (Figure 3).

In the second approach, activation energy is estimated using a calculation formula that considers the energy change involved in a structural change and Gibbs free energy. The structural change energy is the amount of energy necessary to reconstruct the structure of a system from the beginning to the end state without affecting the electronic state.

The physical meaning of the energy of the structure change is the amount of energy required to convert the configuration of the nucleus of the reactants to the configuration of the product core without any change in the electronic state. The maximum electron transfer velocity occurs when the opposite energy equals the energy free of the structure change. Free energy is negative for spontaneous electron transfer, and structure change energy is positive. At this point, the sum of these two numbers is zero. According to the square formula, this sum with a negative sign causes the speed constant to be maximum.

3. Results and discussion

It is feasible to determine the values of ΔG_{et}(1) # to ΔG_{et}(4)#of [β-CD]@[C_n] supramolecular complexes using the equations (Eq. 1-4) utilized in this modeling. The equations (1-2) [39] are used to compute ΔG_{et}(n)# (n=1-4) for [β-CD]@[C_n] supramolecular complexes of C_n where (n=60, 70, 76, 82, 86, 78, 84, 120, 132, 140, 146, 150, 160, 162, 240, 276, 288 and 300). The electron transfer energies of ΔG_{et}(n)# (n=1-4) of the complexes between β -CD derivatives and fullerenes like C_n (n=60, 70, 76, 82, 86, 78, 84, 120, 132, 140, 146, 150, 160, 162, 240, 276, 288 and 300) were estimated calculated based on these data (Table 1-3). The equations were used to explain the estimated values of free electron transfer energies ΔG_{et}(n)# (n=1-4) for the selected [β-CD]@[C_n] supramolecular complexes (n = 60, 70, 76, 82, and 86). Table 1 shows that the approximated and estimated values were inconsistent with the result. The values of ΔG_{et}(n#) (n=1-4) drop as the number of carbon atoms in the fullerene structure rises. The complex supramolecular systems presented here and the computed values of ΔG_{et}(n)# (n=1-4) have never been synthesized or published.

In this regard, due to their ability to form these complexes, cyclodextrins used pharmaceutical and chemical sensors. The composed complexes increase the physical and chemical stability of the drug and allow it to be available for biological systems, especially for low-soluble or insoluble drugs in water [41, 42]. Therefore, it can provide a drug delivery system with controlled and targeted release, greatly benefiting from the properties mentioned above.

*Curves are related to C_n complexes. β-CD (n=1-4) is related to the curve corresponding to the C_n complex.

Estimating the values of ΔGet(n), n=1–4, of [β-CD] is essential in this study. C_n using Eq. 1-3. The estimated free energy values of the transfer of electrons (ΔG_{et}(n), n=1–4, in kcal /mol) between the β-CD and fullerenes C_n in the complexes are shown in Tables 2 and 3. The ΔG_{et}(n) values for [-CD] (n=1–4). Eq. 1-3 and the Rehm-Weller equation estimate C_n (n=60, 70, 76, 82, 86, 78, 84, 120). (Eq.1, Table 3).

These equations establish the correlation between the number of carbon atoms in fullerenes and the first to the fourth free energy of electron transfer for such supramolecular complexes [β-CD.C_n]. All diagrams have been developed using the MATLAB-7.4.0 and Excel 2016 Microsoft Office programs presented in Figures 4 and 5.

As mentioned before, cyclodextrin structures, particularly β-CD, can enhance drug solubility and stability by generating solid-state complex-

es, frequently used in pharmaceutical applications [16]. Electron transport increases as the number of electrons in the C_n structure grow. These results depend on the levels of HOMO and LUMO. The values obtained also point to the negative energy values of the complexes and conductance properties. This work reported the electrochemical data of these selective chemical carriers and fullerenes (supermolecule complexes).

All equations with values are listed in Table 3. the electron transfer energy between the specified transporters and the fullerene structures have been computed in Tables 1-3 to use these results (Equations 1-4) and the Rehm-Weller equation (Eq.1). The calculated values of free energy of electron transfer for these molecular cloud sets are shown in the equations and equations of Rehm-Weller in Table 3. After the calculations were performed and the predicted values were matched favorably. Electron transfer appears to increase as the electron population in the C_n structures increases (Table 3), which is related to the HOMO and LUMO gap of the fullerenes. These results depend on the level of HOMO and LUMO fullerenes. The above analysis shows that designed systems are good candidates for medical applications. A similar report is present in the valuable literature suggesting that designed systems expressed practical medical and pharmaceutical applications. Presenting a model for quantitative communication of structure and free energy activity of electron exchange at the nanoscale in the compounds introduced in this project. Also, to use mathematical methods to correlate several chemical properties.

4. Conclusions

Cyclodextrin compounds, despite having hydrophobic holes in their structure, are water-soluble. Different molecules can enter these holes to form new compounds called tangled complexes. In turn, this led to the developing of medical and pharmaceutical application systems. Topological indicators generally indicate the relationship between chemical structures and physicochemical properties. Computational methods have been used successfully to prove the relationship and dependence between the structure and physicochemical characteristics of these advanced materials. This report highlights the number of carbons in fullerenes as an indicator of communication between β-CD compound and fullerenes. The redox systems and molecular conductors have been identified as key electron transfer qualities. Calculations are presented [β –CD]. C_n supramolecular complexes data by applying equations in the methods used in this study with a good approximation were reported.

The results include the four free energies of electron transfer ($\Delta G_{et}(1)$ to $\Delta G_{et}(4)$), which were calculated using the Rehm-Weller equation and $\Delta G^{\#}_{et}(n)$ as well as $\lambda_{et}(n)$ (n = 1–4) using the Marcus theory equations for the supramolecular complexes between the selected β-CD and the fullerenes.

Conflict of interest statement

All authors declare no conflicts of interest in this paper.

Associated Content

Data supporting to above findings are available on request.

Acknowledgments

The authors thank the Laboratory of Iran University of Science and Technology, Guilan University, and the University of Okara for financial support of this work.

REFERENCES

[1] H. Sahrayi, E. Hosseini, S. Karimifard, N. Khayam, S.M. Meybodi, S. Amiri, M. Bourbour, B. Farasati Far, I. Akbarzadeh, M. Bhia, C. Hoskins, C. Chaiyasut, Co-Delivery of Letrozole and Cyclophosphamide via Folic Acid-Decorated Nanoniosomes for Breast Cancer Therapy: Synergic Effect, Augmentation of Cytotoxicity, and Apoptosis Gene Expression, Pharmaceuticals, 2022.

[2] C. Muankaew, T. Loftsson, Cyclodextrin-Based Formulations: A Non-Invasive Platform for Targeted Drug Delivery, Basic & Clinical Pharmacology & Toxicology 122(1) (2018) 46-55.

[3] F. Eshrati Yeganeh, A. Eshrati Yeganeh, M. Fatemizadeh, B. Farasati Far, S. Quazi, M. Safdar, In vitro cytotoxicity and anti-cancer drug release behavior of methionine-coated magnetite nanoparticles as carriers, Medical Oncology 39(12) (2022) 252.

[4] B. Farasati Far, S. Asadi, M.R. Naimi-Jamal, W.K. Abdelbasset, A. Aghajani Shahrivar, Insights into the interaction of azinphos-methyl with bovine serum albumin: experimental and molecular docking studies, Journal of Biomolecular Structure and Dynamics 40(22) (2022) 11863-11873.

[5] M.A. Przybyla, G. Yilmaz, C.R. Becer, Natural cyclodextrins and their derivatives for polymer synthesis, Polymer Chemistry 11(48) (2020) 7582-7602.

[6] S. Choudhary, L. Gupta, S. Rani, K. Dave, U. Gupta, Impact of Dendrimers on Solubility of Hydrophobic Drug Molecules, 8 (2017).

[7] A. Celebioglu, T. Uyar, Hydrocortisone/cyclodextrin complex electrospun nanofibers for a fast-dissolving oral drug delivery system, RSC Medicinal Chemistry 11(2) (2020) 245-258.

[8] Y.-A. Choi, B.R. Chin, D.H. Rhee, H.-G. Choi, H.-W. Chang, J.-H. Kim, S.-H. Baek, Methyl-β-cyclodextrin inhibits cell growth and cell cycle arrest via a prostaglandin E(2) independent pathway, Experimental & Molecular Medicine 36(1) (2004) 78-84.

[9] A. Stasiłowicz, E. Tykarska, N. Rosiak, K. Sałat, A. Furgała-Wojas, T. Plech, K. Lewandowska, K. Pikosz, K. Pawłowicz, J. Cielecka-Piontek, The Inclusion of Tolfenamic Acid into Cyclodextrins Stimulated by Microenvironmental pH Modification as a Way to Increase the Anti-Migraine Effect, Journal of Pain Research 14 (2021) 981-992.

[10] P. Berben, J. Stappaerts, M.J.A. Vink, E. Domínguez-Vega, G.W. Somsen, J. Brouwers, P. Augustijns, Linking the concentrations of itraconazole and 2-hydroxypropyl-β-cyclodextrin in human intestinal fluids after oral intake of Sporanox®, European Journal of Pharmaceutics and Biopharmaceutics 132 (2018) 231-236.

[11] Y. Xu, C. Zhang, X. Zhu, X. Wang, H. Wang, G. Hu, Q. Fu, Z. He, Chloramphenicol/sulfobutyl ether-β-cyclodextrin complexes in an ophthalmic delivery system: prolonged residence time and enhanced bioavailability in the conjunctival sac, Expert Opinion on Drug Delivery 16(6) (2019) 657-666.

[12] S.S. Braga, Cyclodextrins: Emerging Medicines of the New Millennium, Biomolecules, 2019.

[13] M.H. Asim, M. Ijaz, A. Mahmood, P. Knoll, A. Jalil, S. Arshad, A. Bernkop-Schnürch, Thiolated cyclodextrins: Mucoadhesive and permeation enhancing excipients for ocular drug delivery, International Journal of Pharmaceutics 599 (2021) 120451.

[14] P.C.S. Costa, J.S. Evangelista, I. Leal, P.C.M.L. Miranda, Chemical graph theory for property modeling in QSAR and QSPR—charming QSAR & QSPR, Mathematics 9(1) (2020) 60.

[15] Z. Foroutan, A.R. Afshari, Z. Sabouri, A. Mostafapour, B.F. Far, M. Jalili-Nik, M. Darroudi, Plant-based synthesis of cerium oxide nanoparticles as a drug delivery system in improving the anticancer effects of free temozolomide in glioblastoma (U87) cells, Ceramics International 48(20) (2022) 30441-30450.

[16] F. Eshrati Yeganeh, A. Eshrati Yeganeh, M. Fatemizadeh, B. Farasati Far, S. Quazi, M.J.M.O. Safdar, In vitro cytotoxicity and anti-cancer drug release behavior of methionine-coated magnetite nanoparticles as carriers, 39(12) (2022) 252.

[17] F. Ban, K. Dalal, H. Li, E. LeBlanc, P.S. Rennie, A. Cherkasov, Best Practices of Computer-Aided Drug Discovery: Lessons Learned from the Development of a Preclinical Candidate for Prostate Cancer with a New Mechanism of Action, Journal of Chemical Information and Modeling 57(5) (2017) 1018-1028.

[18] K. Elaheh, G. Nosrat, Potential applications of nanoshell bow-tie antennas for biological imaging and hyperthermia therapy, Optical Engineering 58(6) (2019) 065102.

[19] I. Hdoufane, D. Ounaissi, A. Dermoune, D. Cherqaoui, Development of QSAR Models Using Singular Value Decomposition Method: A Case Study for Predicting Anti-HIV-1 and Anti-HCV Biological Activities, Biointerface Research in Applied Chemistry 12(3) (2021) 3090-3105.

[20] H. Shen, The compressive mechanical properties of Cn (n=20, 60, 80, 180) and endohedral M@C60 (M=Na, Al, Fe) fullerene molecules, Molecular Physics 105(17-18) (2007) 2405-2409.

[21] F. Lu, E.A. Neal, T. Nakanishi, Self-Assembled and Nonassembled Alkylated-Fullerene Materials, Accounts of Chemical Research 52(7) (2019) 1834-1843.

[22] L. Kavan, L. Dunsch, H. Kataura, Electrochemical tuning of electronic struc-

ture of carbon nanotubes and fullerene peapods, Carbon 42(5) (2004) 1011-1019 .
[23] N. Kamanina, Fullerenes and Relative Materials: Properties and Applications, IntechOpen2018.
[24] R.E. Haufler, J. Conceicao, L.P.F. Chibante, Y. Chai, N.E. Byrne, S. Flanagan, M.M. Haley, S.C. O'Brien, C. Pan, et al., Efficient production of C60 (buckminsterfullerene), C60H36, and the solvated buckide ion, The Journal of Physical Chemistry 94(24) (1990) 8634-8636.
[25] P.A. Maggard, X. Cheng, S. Deng, M.-H. Whangbo, Physical Properties of Molecules and Condensed Materials Governed by Onsite Repulsion, Spin-Orbit Coupling and Polarizability of Their Constituent Atoms, Molecules 25(4) (2020) 867.
[26] R. Otero, A.L. Vázquez de Parga, J.M. Gallego, Electronic, structural and chemical effects of charge-transfer at organic/inorganic interfaces, Surface Science Reports 72(3) (2017) 105-145.
[27] R. Purchase, H.J.I.F. De Groot, Biosolar cells: global artificial photosynthesis needs responsive matrices with quantum coherent kinetic control for high yield, 5(3) (2015) 20150014.
[28] M. Najafpour, Applied Photosynthesis: New Progress, IntechOpen2016.
[29] S.-J. Huang, Y.-T. Hsu, Faithful derivation of symmetry indicators: A case study for topological superconductors with time-reversal and inversion symmetries, Physical Review Research 3(1) (2021) 013243.
[30] X. Chen, L. Chen, S. Zheng, H. Wang, Y. Dai, Z. Chen, R. Huang, Disrupted Brain Connectivity Networks in Aphasia Revealed by Resting-State fMRI, 13 (2021).
[31] L. Wang, X. Xue, X. Zhou, Z. Wang, R. Liu, Analyzing the topology characteristic and effectiveness of the China city network, Environment and Planning B: Urban Analytics and City Science 48(9) (2021) 2554-2573.
[32] A.A. Taherpour, D. Narian, A. Taherpour, Structural relationships and theoretical study of the free energies of electron transfer, electrochemical properties, and electron transfer kinetic of cephalosporin antibiotics derivatives with fullerenes in nanostructure of [R]·Cn(R = cefadroxil, cefepime, cephalexin, cefotaxime, cefoperazone and ceftriaxone) supramolecular complexes, Journal of Nanostructure in Chemistry 5(2) (2015) 153-167.
[33] A. Taherpour, M. Maleki-Noureini, Free Energies of Electron Transfer, Electron Transfer Kinetic Theoretical and Quantitative Structural Relationships and Electrochemical Properties Studies of Gadolinium Nitride Cluster Fullerenes Gd3N@Cn in [X-UT-Y][Gd3N@Cn](n = 80, 82, 84, 86 and 88) Supramolecular Complexes, Fullerenes, Nanotubes and Carbon Nanostructures 21(6) (2013) 485-502.
[34] H.R.A. El-Mageed, F.M. Mustafa, M.K. Abdel-Latif, Boron nitride nanoclusters, nanoparticles and nanotubes as a drug carrier for isoniazid anti-tuberculosis drug, computational chemistry approaches, Journal of Biomolecular Structure and Dynamics 40(1) (2022) 226-235.
[35] B. Farasati Far, M.R. Naimi-Jamal, M. Jahanbakhshi, H.T. Mohammed, U.S. Altimari, J. Ansari, Poly(3-thienylboronic acid) coated magnetic nanoparticles as a magnetic solid-phase adsorbent for extraction of methamphetamine from urine samples, Journal of Dispersion Science and Technology (2022) 1-11.
[36] B. Farasati Far, D. Bokov, G. Widjaja, H. Setia Budi, W. Kamal Abdelbasset, S. Javanshir, F. Seif, H. Pazoki-Toroudi, S.K. Dey, Metronidazole, acyclovir and tetrahydrobiopterin may be promising to treat COVID-19 patients, through interaction with interleukin-12, Journal of Biomolecular Structure and Dynamics (2022) 1-19.
[37] C.A. Celaya, J. Muñiz, L.E. Sansores, New nanostructures of carbon: Quasi-fullerenes Cn-q (n=20, 42, 48, 60), Computational and Theoretical Chemistry 1117 (2017) 20-29.
[38] C. Bannwarth, S. Ehlert, S. Grimme, GFN2-xTB—An Accurate and Broadly Parametrized Self-Consistent Tight-Binding Quantum Chemical Method with Multipole Electrostatics and Density-Dependent Dispersion Contributions, Journal of Chemical Theory and Computation 15(3) (2019) 1652-1671.
[39] R.A.J.T.J.o.c.p. Marcus, On the theory of oxidation-reduction reactions involving electron transfer. I, 24(5) (1956) 966-978.
[40] A.T. Avat, A.-R. Shafaati, Theoretical Study of Structural Relationships and Electrochemical Properties of [DNA-Nucleotide Bases]@ Cn Complexes, Oriental Journal of Chemistry 27(3) (2011) 823.
[41] B. Farasati Far, K. Vakili, M. Fathi, S. Yaghoobpoor, M. Bhia, M.R. Naimi-Jamal, The role of microRNA-21 (miR-21) in pathogenesis, diagnosis, and prognosis of gastrointestinal cancers: A review, Life Sciences 316 (2023) 121340.
[42] B. Farasati Far, S. Asadi, M.R. Naimi-Jamal, W.K. Abdelbasset, A.J.J.o.B.S. Aghajani Shahrivar, Dynamics, Insights into the interaction of azinphos-methyl with bovine serum albumin: Experimental and molecular docking studies, 40(22) (2022) 11863-11873.